

The LS89 Optimization Test Case

Lasse Mueller, Tom Verstraete

March 1, 2016

Abstract

This document describes the LS89 axial turbine optimization test case, specifically designed to challenge modern design optimization systems. The baseline profile is the VKI LS89 profile which has an extensive experimental database to validate CFD codes. Whilst the datum blade profile was initially designed and optimized for subsonic flows, we propose three different test cases ranging from a single-point optimization at transonic flow conditions to two different multi-point optimization setups including sub- and transonic flow at different inlet flow angles.

This document describes the full set up of the optimization problem, as well as the necessary experimental data to validate the CFD solver on the baseline geometry.

1 The LS89 Test Case

The LS98 test case is one of the notorious turbine test cases which is frequently used to benchmark the aero-thermal predictive capabilities of CFD codes. The LS89 test campaign was initiated in a period witnessing a remarkable progress in the development of reliable CFD codes. The efforts made at the *von Karman Institute for Fluid Dynamics* (VKI) were particularly aimed in response to the conclusions of the AGARD Working Group 18 [5], which stated that further detailed test cases providing more information on boundary layer characteristics were necessary for validating numerical Navier-Stokes codes.

The LS89 blade profile is a high pressure turbine nozzle guide vane representative of modern aero-engines. The blade shape was optimized for a downstream isentropic Mach number equal to 0.9 by means of an inverse method [4], developed at the VKI. The blade profile, as well as the optimization test cases in this report are two-dimensional.

A preliminary set of results on the LS89 test case was presented during the Lecture Series on "Numerical Methods for Flows in Turbomachinery" [3] held at the VKI in May 1989, and compared to the numerical predictions provided by a number of participants. The complete experimental results were then published during the 1990 International Gas Turbine Conference held in Brussels [1]. The final report, on which this document is based is the VKI Technical Note TN174 [2].

2 The LS89 Baseline Geometry

The two-dimensional geometry of the LS89 blade is shown in Fig. 1 and its main geometrical parameters are listed in Tab. 1. This geometry serves as the baseline geometry for all test cases in this report and should be used to validate the CFD solver for the test conditions defined in Sec. 3.

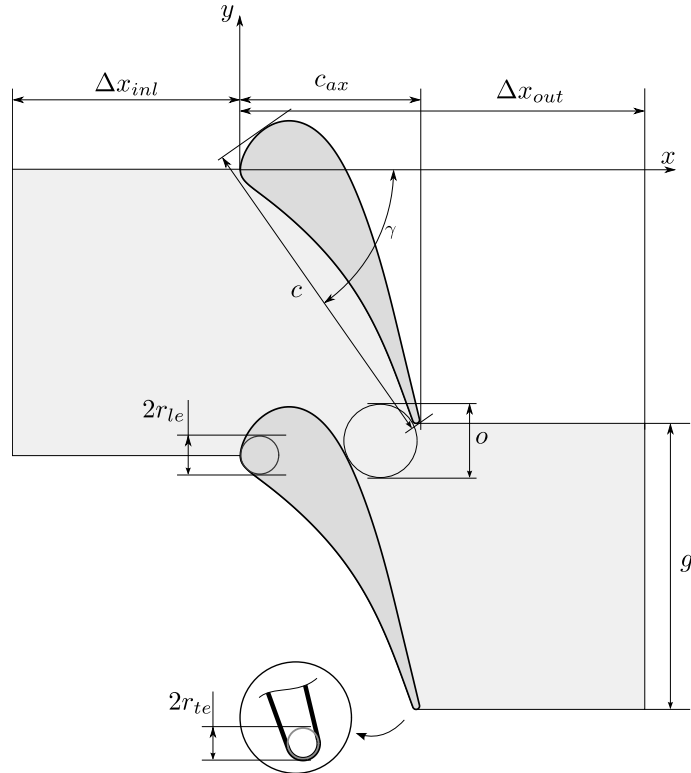


Figure 1: Definition of the geometrical characteristics of the LS89 blade (Not to scale).

The profile geometry itself is available in different formats. The most common format to exchange profile shapes is through a discretized set of x-y-coordinates along the suction and pressure side. The coordinates are tabulated and represented in Tab. 9 from TN174 [2].

Although a large number of points has been used along the suction and pressure side, point data is known to introduce noise, which is particularly present in the data of Tab. 9. As an alternative, we provide the shape of the profile through the control points of two Bézier curves defining the suction and pressure side of the blade. The x-y-coordinates of the control points are listed in Tab. 2. The shape is closed by a circular trailing edge defined by Tab. 3. A view on the position of the control points of the respective curves is given in Fig. 2.

Parameter		Value
Chord	c	67.647 mm
Pitch	g	57.500 mm
Throat	o	14.930 mm
LE radius	r_{le}	4.127 mm
TE radius	r_{te}	0.710 mm
Axial chord	c_{ax}	36.985 mm
Inlet length	Δx_{inl}	55.0 mm
Outlet length	Δx_{out}	64.0 mm
Stagger angle	γ	55°

Table 1: Geometrical parameters of the LS89 blade defined in Fig. 1.

Index -	SS		PS	
	x mm	y mm	x mm	y mm
1	0.000	0.000	0.000	0.000
2	0.000	5.149	0.000	-4.643
3	7.010	16.026	6.095	-3.510
4	13.848	12.910	9.429	-10.969
5	22.525	12.270	18.394	-14.941
6	19.524	-2.086	25.999	-23.767
7	26.745	-4.241	30.093	-36.793
8	25.599	-13.085	35.578	-51.863
9	30.812	-17.997		
10	30.111	-26.464		
11	32.828	-33.844		
12	34.732	-42.274		
13	36.936	-51.453		

Table 2: Coordinates of the Bézier control points of the suction and pressure side curves.

Radius mm	x mm	y mm
0.710	-36.245	-51.620

Table 3: Radius and coordinates of the center point of trailing edge circle.

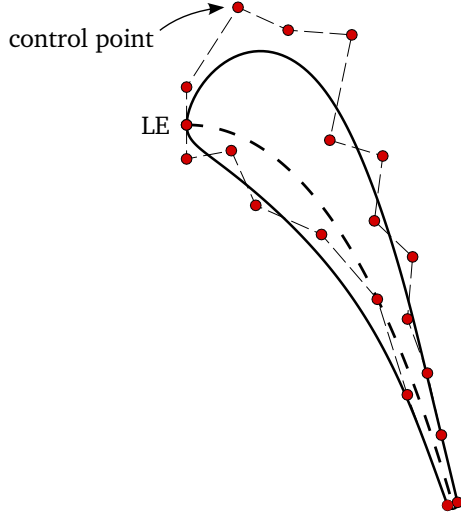


Figure 2: Position of the Bézier control points of the suction and pressure side.

Inlet total temperature	T_{01}	420 K
Inlet total pressure	P_{01}	$1.596 \cdot 10^5$ Pa
Inlet flow angle	α_1	0.0°
Inlet turbulence intensity	Tu_∞	3
Outlet static pressure	P_2	$0.8235 \cdot 10^5$ Pa

Table 4: Boundary conditions for the MUR47 test conditions

3 The MUR47 Test Conditions

The TN174 [2] specifies experimental results for a large number of test conditions in which Reynolds number, Mach number and turbulence intensity are independently varied. In addition to the isentropic Mach number distribution, further data is available such as losses and exit flow angles but also heat transfer measurements. We however focus only on the isentropic Mach number distribution to validate the CFD solver, which is defined as follows

$$M_{is} = \sqrt{\frac{2}{\gamma - 1} \left[\left(\frac{P_{01}}{P} \right)^{\frac{\gamma-1}{\gamma}} - 1 \right]} \quad (1)$$

where P_{01} is the inlet total pressure and P the static pressure on the blade surface. The ratio of specific heats γ is given in Tab. 5.

The boundary conditions for the MUR47 test case are listed in Tab. 4. These conditions correspond to an isentropic exit Mach number of 1.02 and a Reynolds number of 10^6 . At the inlet the total pressure, total temperature and flow angles are prescribed while at the outlet a constant static pressure is imposed. The blade surface is considered adiabatic.

The working fluid is air modeled as a perfect caloric gas, with properties

Name		Value	Unit
Gas constant	R	287	J/(kg.K)
Ratio of specific heats	γ	1.4	—
Prandtl number	Pr	0.7	—
Reference dynamic viscosity	μ_{ref}	$1.716 \cdot 10^{-5}$	kg/(s.m)
Reference temperature	T_{ref}	273.15	K
Sutherland temperature	S	110.4	K

Table 5: Properties of air.

summarized in Tab. 5. Sutherlands's law is used to compute the laminar viscosity

$$\mu = \mu_{ref} \left(\frac{T}{T_{ref}} \right)^{3/2} \frac{T_{ref} + S}{T + S} \quad (2)$$

The measured isentropic Mach number distribution on the suction and pressure side is listed in Tab. 6. The inlet total pressure P_{01} is used as reference pressure while the position of the pressure taps on the blade is measured in axial direction.

SS		PS	
x mm	Is. Mach	x mm	Is. Mach
0.000	0.000	0.603	0.036
0.293	0.088	2.087	0.049
1.051	0.167	6.816	0.107
5.070	0.438	14.375	0.145
11.500	0.704	23.111	0.209
14.653	0.844	29.544	0.378
17.250	0.892	33.757	0.657
19.336	0.907		
22.690	1.006		
24.854	1.045		
26.037	1.066		
27.122	1.105		
28.509	1.141		
29.435	1.183		
30.326	1.216		
31.996	1.203		
33.589	1.071		
35.179	0.960		
36.355	0.999		
36.461	0.875		

Table 6: Isentropic Mach number distribution on the suction and pressure side for test condition MUR47.

4 Optimization Test Case 1

The first test case considers a single-point optimization at transonic flow conditions.

4.1 Boundary Conditions

The boundary conditions of this test case correspond to the previously defined ones of MUR47 in Sec. 3, which are listed in Tab. 4. These conditions result in a slightly higher Mach number than the original design intend of the LS89 blade, such that now the operation becomes transonic characterized by a strong normal shock on the rear part of the suction side of the blade. Large improvements are to be expected especially attributed to reduced shock losses by changing the shape of the rear part of the suction side.

4.2 Shape Parameters

A large degree of freedom is given to the shape variation during the optimization process. The suction and pressure side curves are allowed to change fully independently from each other. Additionally the pitch g (see Fig. 1) is a free parameter, as well as the stagger angle γ , the geometrical throat o and the leading edge radius r_{le} of the blade.

However, the trailing edge radius r_{te} and the axial chord length of the blade need to remain fixed. Note the solidity (c/g) can still be changed through changing the pitch. No constraint is imposed on minimal thickness.

4.3 Objective

The objective of this optimization is to minimize the mass-flow averaged entropy production in the cascade and is defined as:

$$\Delta \tilde{s} = \frac{\tilde{s}_{out} - \tilde{s}_{in}}{s_{ref}} \quad (3)$$

with the mass-flow averaged entropy ($s = P/\rho^\gamma$)

$$\tilde{s} = \frac{\int\limits_{y=0}^{y=g} \rho \cdot V_x(y) \cdot s \, dy}{\int\limits_{y=0}^{y=g} \rho \cdot V_x(y) \, dy}. \quad (4)$$

The evaluation planes where the integral values are calculated are the inlet and outlet of the computational domain as illustrated in Fig. 1 ($x = -\Delta x_{in}, x = \Delta x_{out}$). The reference entropy $s_{ref} = P_{01}/\rho_{01}^\gamma$ in Eqn. 3 is computed with the total inlet conditions according to Tab. 4.

Operating point	P_2
1	$0.94365 \cdot 10^5$ Pa
2	$0.82356 \cdot 10^5$ Pa
3	$0.74749 \cdot 10^5$ Pa

Table 7: Exit boundary conditions for test case 2

4.4 Constraint

Without imposing any constraint the optimizer will unload the blade by reducing the flow turning inside the blade passage. For this reason a constraint is imposed on the exit flow angle:

$$\alpha_2 \geq 74^\circ \quad (5)$$

where α_2 is defined as the mass-flow averaged exit flow angle with respect to axial direction

$$\alpha_2 = \frac{\int_{y=0}^{y=g} \rho \cdot V_x(y) \cdot \text{atan} \left(-\frac{V_y(y)}{V_x(y)} \right) dy}{\int_{y=0}^{y=g} \rho \cdot V_x(y) dy} \quad (6)$$

5 Optimization Test Case 2

The second test case considers a multi-point optimization in which the operating exit Mach number is varied.

5.1 Boundary conditions

Three different operating points are considered, corresponding to an exit isentropic Mach numbers of 0.9, 1.02 and 1.1 respectively. The inlet conditions remain the one of MUR47, listed in Tab. 4. The static pressure at the exit of the domain for the three different operating conditions is given by Tab. 7

5.2 Shape parameters

The same degree of freedom is given as in test case 1 (see SubSec. 4.2).

5.3 Objective

The objective of this optimization is to minimize the weighted sum of mass-flow averaged entropy production in the cascade and is defined as:

$$\Delta \tilde{s} = \frac{\Delta \tilde{s}^{op1} + \Delta \tilde{s}^{op2} + \Delta \tilde{s}^{op3}}{3} \quad (7)$$

where the entropy generation of the individual operating points is computed by Eqn. 3.

Operating point	α_1	P_2
1	0°	$0.94365 \cdot 10^5$ Pa
2	-30°	$0.82356 \cdot 10^5$ Pa
3	0°	$0.82356 \cdot 10^5$ Pa
4	30°	$0.82356 \cdot 10^5$ Pa
5	0°	$0.74749 \cdot 10^5$ Pa

Table 8: Exit boundary conditions for test case 3

5.4 Constraint

The same constraint as for test case 1 is imposed, but to each individual operating point. This results in three constraints:

$$\alpha_2^{op_i} \geq 74^\circ \quad i \in [1, 3] \quad (8)$$

where α_2 is defined by Eqn.6.

6 Optimization Test Case 3

The third test case considers a multi-point optimization in which the operating exit Mach number and inlet flow angle are varied.

6.1 Boundary conditions

In total five different operating points are considered, corresponding to an exit isentropic Mach numbers of 0.9, 1.02 and 1.1, and for which the inlet flow angle is changed between -30°, 0° and 30°. The remaining inlet conditions are the one of MUR47, listed in Tab. 4. The boundary conditions for the five operating conditions are given by Tab. 8

6.2 Shape parameters

The same degree of freedom is given as in test case 1 (see SubSec. 4.2).

6.3 Objective

The objective of this optimization is to minimize the weighted sum of mass averaged entropy production in the cascade and is defined as:

$$\Delta\tilde{s} = \frac{\Delta\tilde{s}^{op1} + \Delta\tilde{s}^{op2} + \Delta\tilde{s}^{op3} + \Delta\tilde{s}^{op4} + \Delta\tilde{s}^{op5}}{5} \quad (9)$$

where the entropy generation of the individual operating points is computed by Eqn. 3.

6.4 Constraint

The same constraint as for test case 1 is imposed, but to each individual operating point. This results in five constraints:

$$\alpha_2^{op_i} \geq 74^\circ \quad i \in [1, 5] \quad (10)$$

where α_2 is defined by Eqn.6.

7 Conclusions

The present document provides the LS89 profile shape in two different formats, as well as experimental results for the MUR47 test case. It serves as the datum design for any type of optimization algorithm to be applied to. Three different optimization setups are provided.

It is hoped that this document will lead to an increased exchange of data across different research groups, and allow to asses the performance of different CFD based optimization algorithms.

8 References

References

- [1] T. Arts and M. L. de Rouvroit. Aero-Thermal Performance of a Two Dimensional Highly Loaded Transonic Turbine Nozzle Guide Vane - A test case for Inviscid and Viscous Flow Computations. In *ASME TURBO EXPO*, Brussels, Belgium, June 1990. Paper No. 90-GT-358.
- [2] T. Arts, M. L. de Rouvroit, and A. W. Rutherford. Aero-Thermal Investigation of a Highly Loaded Transonic Linear Turbine Guide Vane Cascade - A test case for Inviscid and Viscous Flow Computations. In *VKI Technical Note TN174*, Brussels, Belgium, September 1990.
- [3] T. Arts, M. L. de Rouvroit, and C. H. Sieverding. Contribution to the workshop on two dimensional inviscid and viscous turbomachinery flow calculation. In *V.K.I. Lecture Series 1989-06*, Brussels, Belgium, May 1989.
- [4] R. A. V. den Breembussche, O. Leonard, and L. Nekmouche. Subsonic and Transonic blade design by means of analysis codes. In *64 th FDP specialists' meeting on "Computational Methods for Aerodynamic design (inverse) and optimization"*, Loen, Norway, May 1989.
- [5] L. Fottner. Overview on Test Cases for Computation of Internal Flows in Turbomachines. In *ASME TURBO EXPO*, Torronto, Canada, June 1989. Paper No. 89-GT-46.

9 Appendix

Table 9: Coordinates of the LS89 profile, from [5]

X mm	Y mm	S mm	S/SSS	S/C	X mm	Y mm	S mm	S/SPS	S/C
-	-	-	-	-	-	-	-	-	-
0.000	0.000	0.000	0.000	0.000	0.000	0.000	0.000	0.000	0.000
0.185	1.554	1.565	0.018	0.023	0.185	-0.913	0.932	0.014	0.014
0.371	2.349	2.381	0.028	0.035	0.371	-1.513	1.560	0.024	0.023
0.556	2.850	2.916	0.034	0.043	0.556	-1.858	1.951	0.030	0.029
0.742	3.298	3.401	0.039	0.050	0.742	-2.086	2.245	0.034	0.033
0.927	3.662	3.809	0.044	0.056	0.927	-2.278	2.512	0.038	0.037
1.113	3.982	4.179	0.048	0.062	1.113	-2.467	2.777	0.042	0.041
1.298	4.267	4.519	0.052	0.067	1.298	-2.649	3.037	0.046	0.045
1.484	4.548	4.856	0.056	0.072	1.484	-2.810	3.283	0.050	0.049
1.669	4.825	5.189	0.060	0.077	1.669	-2.963	3.523	0.054	0.052
1.855	5.099	5.520	0.064	0.082	1.855	-3.112	3.761	0.058	0.056
2.040	5.366	5.845	0.068	0.086	2.040	-3.260	3.998	0.061	0.059
2.226	5.618	6.158	0.071	0.091	2.226	-3.407	4.235	0.065	0.063
2.411	5.859	6.462	0.075	0.096	2.411	-3.554	4.471	0.068	0.066
2.597	6.095	6.762	0.078	0.100	2.597	-3.703	4.710	0.072	0.070
2.782	6.326	7.058	0.082	0.104	2.782	-3.852	4.947	0.076	0.073
2.968	6.549	7.349	0.085	0.109	2.968	-4.001	5.186	0.079	0.077
3.153	6.765	7.633	0.088	0.113	3.153	-4.150	5.423	0.083	0.080
3.339	6.971	7.911	0.091	0.117	3.339	-4.299	5.661	0.087	0.084
3.524	7.166	8.179	0.095	0.121	3.524	-4.448	5.899	0.090	0.087
3.710	7.351	8.442	0.098	0.125	3.710	-4.596	6.137	0.094	0.091
3.895	7.524	8.695	0.101	0.129	3.895	-4.746	6.375	0.098	0.094
4.081	7.688	8.943	0.103	0.132	4.081	-4.895	6.613	0.101	0.098
4.266	7.843	9.184	0.106	0.136	4.266	-5.044	6.851	0.105	0.101
4.452	7.987	9.420	0.109	0.139	4.452	-5.194	7.090	0.108	0.105
4.637	8.122	9.649	0.112	0.143	4.637	-5.343	7.327	0.112	0.108
4.822	8.251	9.874	0.114	0.146	4.822	-5.493	7.565	0.116	0.112
5.008	8.372	10.096	0.117	0.149	5.008	-5.643	7.804	0.119	0.115
5.193	8.486	10.313	0.119	0.152	5.193	-5.793	8.043	0.123	0.119
5.379	8.594	10.528	0.122	0.156	5.379	-5.944	8.282	0.127	0.122
5.564	8.698	10.741	0.124	0.159	5.564	-6.094	8.520	0.130	0.126
5.750	8.798	10.952	0.127	0.162	5.750	-6.245	8.760	0.134	0.129
5.935	8.895	11.161	0.129	0.165	5.935	-6.396	8.999	0.138	0.133
6.121	8.987	11.368	0.131	0.168	6.121	-6.547	9.238	0.141	0.137
6.306	9.077	11.574	0.134	0.171	6.306	-6.699	9.478	0.145	0.140
6.492	9.164	11.779	0.136	0.174	6.492	-6.851	9.718	0.149	0.144
6.677	9.248	11.983	0.139	0.177	6.677	-7.003	9.957	0.152	0.147
6.863	9.326	12.184	0.141	0.180	6.863	-7.156	10.198	0.156	0.151
7.048	9.400	12.383	0.143	0.183	7.048	-7.309	10.438	0.160	0.154
7.234	9.469	12.582	0.146	0.186	7.234	-7.463	10.680	0.163	0.158
7.419	9.533	12.778	0.148	0.189	7.419	-7.616	10.920	0.167	0.161
7.605	9.591	12.972	0.150	0.192	7.605	-7.771	11.162	0.171	0.165

Table 9: Coordinates of the LS89 profile (continued).

X mm	Y mm	S mm	S/SSS	S/C	X mm	Y mm	S mm	S/SPS	S/C
		-	-	-			-	-	-
7.790	9.644	13.165	0.152	0.195	7.790	-7.926	11.403	0.174	0.169
7.976	9.691	13.357	0.154	0.197	7.976	-8.081	11.645	0.178	0.172
8.161	9.732	13.546	0.157	0.200	8.161	-8.237	11.887	0.182	0.176
8.347	9.770	13.736	0.159	0.203	8.347	-8.393	12.130	0.186	0.179
8.532	9.804	13.924	0.161	0.206	8.532	-8.550	12.373	0.189	0.183
8.718	9.833	14.112	0.163	0.209	8.718	-8.707	12.616	0.193	0.186
8.903	9.859	14.299	0.165	0.211	8.903	-8.865	12.859	0.197	0.190
9.089	9.880	14.486	0.168	0.214	9.089	-9.023	13.103	0.201	0.194
9.274	9.898	14.672	0.170	0.217	9.274	-9.182	13.347	0.204	0.197
9.460	9.912	14.859	0.172	0.220	9.460	-9.342	13.593	0.208	0.201
9.645	9.923	15.044	0.174	9.645	0.222	-9.502	13.837	0.212	0.205
9.830	9.931	15.229	0.176	0.225	9.830	-9.663	14.083	0.216	0.208
10.016	9.936	15.415	0.178	0.228	10.016	-9.824	14.329	0.219	0.212
10.201	9.938	15.600	0.180	0.231	10.201	-9.987	14.575	0.223	0.215
10.387	9.936	15.786	0.183	0.233	10.387	-10.149	14.822	0.227	0.219
10.572	9.932	15.971	0.185	0.236	10.572	-10.313	15.069	0.231	0.223
10.758	9.923	16.158	0.187	0.239	10.758	-10.476	15.316	0.234	0.226
10.943	9.910	16.343	0.189	0.242	10.943	-10.642	15.565	0.238	0.230
11.129	9.893	16.530	0.191	0.244	11.129	-10.809	15.815	0.242	0.234
11.314	9.871	16.716	0.193	0.247	11.314	-10.978	16.065	0.246	0.237
11.500	9.846	16.904	0.196	0.250	11.500	-11.148	16.317	0.250	0.241
11.685	9.816	17.091	0.198	0.253	11.685	-11.320	16.570	0.254	0.245
11.871	9.783	17.280	0.200	0.255	11.871	-11.491	16.823	0.257	0.249
12.056	9.744	17.469	0.202	0.258	12.056	-11.664	17.076	0.261	0.252
12.242	9.701	17.660	0.204	0.261	12.242	-11.837	17.330	0.265	0.256
12.427	9.652	17.852	0.206	0.264	12.427	-12.010	17.583	0.269	0.260
12.613	9.598	18.045	0.209	0.267	12.613	-12.184	17.838	0.273	0.264
12.799	9.538	18.241	0.211	0.270	12.799	-12.358	18.093	0.277	0.267
12.984	9.473	18.437	0.213	0.273	12.984	-12.534	18.348	0.271	0.281
13.169	9.403	18.635	0.216	0.275	13.169	-12.709	18.603	0.285	0.275
13.355	9.331	18.834	0.218	0.278	13.355	-12.885	18.859	0.289	0.279
13.540	9.253	19.035	0.220	0.281	13.540	-13.062	19.115	0.293	0.283
13.726	9.170	19.238	0.223	0.284	13.726	-13.240	19.372	0.296	0.286
13.911	9.082	19.443	0.225	0.287	13.911	-13.418	19.629	0.300	0.290
14.097	8.987	19.652	0.227	0.291	14.097	-13.597	19.887	0.304	0.294
14.282	8.884	19.864	0.230	0.294	14.282	-13.776	20.145	0.308	0.298
14.467	8.774	20.079	0.232	0.297	14.467	-13.956	20.403	0.312	0.302
14.653	8.660	20.297	0.235	0.300	14.653	-14.137	20.662	0.316	0.305
14.838	8.541	20.517	0.237	0.303	14.838	-14.318	20.921	0.320	0.309
15.024	8.417	20.741	0.240	0.307	15.024	-14.501	21.182	0.324	0.313
15.209	8.289	20.966	0.242	0.310	15.209	-14.686	21.444	0.328	0.317
15.395	8.154	21.196	0.245	0.313	15.395	-14.872	21.707	0.332	0.321
15.580	8.013	21.428	0.248	0.317	15.580	-15.058	21.969	0.336	0.325
15.766	7.866	21.665	0.251	0.320	15.766	-15.247	22.234	0.340	0.329
15.951	7.713	21.905	0.253	0.324	15.951	-15.436	22.499	0.344	0.333

Table 9: Coordinates of the LS89 profile (continued).

X mm	Y mm	S mm	S/SSS	S/C	X mm	Y mm	S mm	S/SPS	S/C
-	-	-	-	-	-	-	-	-	-
16.137	7.554	22.150	0.256	0.327	16.137	-15.627	22.765	0.348	0.337
16.322	7.392	22.396	0.259	0.331	16.322	-15.819	23.032	0.352	0.340
16.508	7.226	22.645	0.262	0.335	16.508	-16.012	23.300	0.357	0.344
16.693	7.053	22.899	0.265	0.339	16.693	-16.208	23.569	0.361	0.348
16.879	6.874	23.157	0.268	0.342	16.879	-16.405	23.840	0.365	0.352
17.064	6.686	23.420	0.271	0.346	17.064	-16.603	24.111	0.369	0.356
17.250	6.490	23.691	0.274	0.350	17.250	-16.803	24.384	0.373	0.360
17.436	6.287	23.966	0.277	0.354	17.436	-17.005	24.659	0.377	0.365
17.621	6.078	24.245	0.280	0.358	17.621	-17.208	24.934	0.382	0.369
17.806	5.864	24.528	0.284	0.363	17.806	-17.412	25.209	0.386	0.373
17.992	5.645	24.815	0.287	0.367	17.992	-17.619	25.487	0.390	0.377
18.177	5.422	25.105	0.290	0.371	18.177	-17.828	25.766	0.394	0.381
18.363	5.190	25.402	0.294	0.376	18.363	-18.038	26.047	0.399	0.385
18.548	4.951	25.705	0.297	0.380	18.548	-18.250	26.328	0.403	0.389
18.734	4.705	26.013	0.301	0.385	18.734	-18.465	26.613	0.407	0.393
18.919	4.452	26.326	0.304	0.389	18.919	-18.681	26.897	0.412	0.398
19.105	4.195	26.644	0.308	0.394	19.105	-18.899	27.184	0.416	0.402
19.290	3.933	26.964	0.312	0.399	19.290	-19.120	27.472	0.420	0.406
19.475	3.665	27.290	0.316	0.403	19.475	-19.342	27.761	0.425	0.410
19.661	3.392	27.620	0.319	0.408	19.661	-19.567	28.053	0.429	0.415
19.846	3.112	27.956	0.323	0.413	19.846	-19.794	28.346	0.434	0.419
20.032	2.824	28.299	0.327	0.418	20.032	-20.022	28.640	0.438	0.423
20.217	2.528	28.648	0.331	0.423	20.217	-20.254	28.937	0.443	0.428
20.403	2.226	29.003	0.335	0.429	20.403	-20.488	29.235	0.447	0.432
20.588	1.917	29.363	0.340	0.434	20.588	-20.724	29.535	0.452	0.437
20.774	1.602	29.729	0.344	0.439	20.774	-20.963	29.838	0.457	0.441
20.959	1.282	30.098	0.348	0.445	20.959	-21.204	30.142	0.461	0.446
21.145	0.956	30.474	0.352	0.450	21.145	-21.447	30.448	0.466	0.450
21.330	0.623	30.854	0.357	0.456	21.330	-21.694	30.757	0.471	0.455
21.516	0.284	31.241	0.361	0.462	21.516	-21.943	31.067	0.475	0.459
21.701	-0.062	31.634	0.366	0.468	21.701	-22.195	31.380	0.480	0.464
21.887	-0.415	32.033	0.370	0.474	21.887	-22.449	31.695	0.485	0.469
22.073	-0.772	32.435	0.375	0.479	22.073	-22.707	32.013	0.490	0.473
22.258	-1.135	32.842	0.380	0.485	22.258	-22.966	32.331	0.495	0.478
22.444	-1.503	33.255	0.385	0.492	22.444	-23.229	32.653	0.500	0.483
22.629	-1.880	33.675	0.389	0.498	22.629	-23.496	32.978	0.505	0.488
22.814	-2.266	34.103	0.394	0.504	22.814	-23.764	33.304	0.510	0.492
23.000	-2.663	34.541	0.399	0.511	23.000	-24.036	33.633	0.515	0.497
23.185	-3.068	34.986	0.405	0.517	23.185	-24.312	33.966	0.520	0.502
23.371	-3.480	35.439	0.410	0.524	23.371	-24.591	34.301	0.525	0.507
23.556	-3.896	35.894	0.415	0.531	23.556	-24.872	34.637	0.530	0.512
23.742	-4.314	36.351	0.420	0.537	23.742	-25.157	34.978	0.535	0.517
23.927	-4.735	36.811	0.426	0.544	23.927	-25.445	35.320	0.540	0.522
24.112	-5.163	37.277	0.431	0.551	24.112	-25.737	35.666	0.546	0.527
24.298	-5.598	37.751	0.437	0.558	24.298	-26.032	36.014	0.551	0.532

Table 9: Coordinates of the LS89 profile (continued).

X mm	Y mm	S mm	S/SSS	S/C	X mm	Y mm	S mm	S/SPS	S/C
		-	-	-			-	-	-
24.483	-6.043	38.232	0.442	0.565	24.483	-26.331	36.366	0.556	0.538
24.669	-6.501	38.727	0.448	0.572	24.669	-26.634	36.722	0.562	0.543
24.854	-6.971	39.232	0.454	0.580	24.854	-26.941	37.080	0.567	0.548
25.040	-7.448	39.744	0.460	0.588	25.040	-27.250	37.441	0.573	0.553
25.225	-7.929	40.259	0.466	0.595	25.225	-27.562	37.803	0.578	0.559
25.411	-8.417	40.781	0.472	0.603	25.411	-27.877	38.169	0.584	0.564
25.596	-8.911	41.309	0.478	0.611	25.596	-28.197	38.539	0.590	0.570
25.782	-9.415	41.846	0.484	0.619	25.782	-28.521	38.912	0.595	0.575
25.967	-9.929	42.392	0.490	0.627	25.967	-28.850	39.290	0.601	0.581
26.153	-10.453	42.949	0.497	0.635	26.153	-29.185	39.673	0.607	0.586
26.338	-10.988	43.515	0.503	0.643	26.338	-29.525	40.060	0.613	0.592
26.524	-11.532	44.090	0.510	0.652	26.524	-29.869	40.451	0.619	0.598
26.710	-12.085	44.673	0.517	0.660	26.710	-30.215	40.844	0.625	0.604
26.895	-12.647	45.265	0.524	0.669	26.895	-30.567	41.242	0.631	0.610
27.081	-13.217	45.864	0.530	0.678	27.081	-30.921	41.642	0.637	0.616
27.266	-13.798	46.474	0.538	0.687	27.266	-31.280	42.045	0.643	0.622
27.451	-14.389	47.093	0.545	0.696	27.451	-31.643	42.453	0.650	0.628
27.637	-14.986	47.719	0.552	0.705	27.637	-32.012	42.866	0.656	0.634
27.822	-15.591	48.351	0.559	0.715	27.822	-32.385	43.282	0.662	0.640
28.008	-16.202	48.990	0.567	0.724	28.008	-32.763	43.704	0.669	0.646
28.193	-16.821	49.636	0.574	0.734	28.193	-33.145	44.128	0.675	0.652
28.379	-17.445	50.287	0.582	0.743	28.379	-33.532	44.557	0.682	0.659
28.564	-18.076	50.945	0.589	0.753	28.564	-33.924	44.991	0.688	0.665
28.750	-18.713	51.608	0.597	0.763	28.750	-34.322	45.430	0.695	0.672
28.935	-19.358	52.279	0.605	0.773	28.935	-34.724	45.873	0.702	0.678
29.120	-20.009	52.956	0.612	0.783	29.120	-35.133	46.322	0.709	0.685
29.306	-20.665	53.638	0.620	0.793	29.306	-35.546	46.775	0.716	0.691
29.491	-21.327	54.325	0.628	0.803	29.491	-35.964	47.232	0.723	0.698
29.677	-21.992	55.016	0.636	0.813	29.677	-36.387	47.694	0.730	0.705
29.862	-22.664	55.713	0.644	0.824	29.862	-36.816	48.161	0.737	0.712
30.048	-23.344	56.418	0.653	0.834	30.048	-37.250	48.633	0.744	0.719
30.233	-24.034	57.132	0.661	0.845	30.233	-37.690	49.111	0.752	0.726
30.419	-24.735	57.857	0.669	0.855	30.419	-38.136	49.594	0.759	0.733
30.604	-25.445	58.591	0.678	0.866	30.604	-38.586	50.080	0.766	0.740
30.790	-26.162	59.332	0.686	0.877	30.790	-39.042	50.573	0.774	0.748
30.975	-26.886	60.079	0.695	0.888	30.975	-39.506	51.072	0.782	0.755
31.161	-27.615	60.831	0.704	0.899	31.161	-39.978	51.580	0.789	0.762
31.347	-28.347	61.587	0.712	0.910	31.347	-40.456	52.093	0.797	0.770
31.532	-29.083	62.346	0.721	0.922	31.532	-40.938	52.609	0.805	0.778
31.718	-29.823	63.109	0.730	0.933	31.718	-41.422	53.127	0.813	0.785
31.903	-30.566	63.874	0.739	0.944	31.903	-41.909	53.648	0.821	0.793
32.089	-31.312	64.643	0.748	0.956	32.089	-42.398	54.171	0.829	0.801
32.274	-32.064	65.418	0.757	0.967	32.274	-42.890	54.697	0.837	0.809
32.459	-32.820	66.196	0.766	0.979	32.459	-43.387	55.227	0.845	0.816
32.645	-33.585	66.983	0.775	0.990	32.645	-43.891	55.765	0.853	0.824

Table 9: Coordinates of the LS89 profile (continued).

X mm	Y mm	S mm	S/SSS	S/C	X mm	Y mm	S mm	S/SPS	S/C
-	-	-	-	-	-	-	-	-	-
32.830	-34.362	67.782	0.784	1.002	32.830	-44.395	56.301	0.862	0.832
33.016	-35.130	68.572	0.793	1.014	33.016	-44.901	56.841	0.870	0.840
33.201	-35.897	69.361	0.802	1.025	33.201	-45.405	57.377	0.878	0.848
33.387	-36.665	70.151	0.811	1.037	33.387	-45.911	57.917	0.886	0.856
33.572	-37.432	70.940	0.820	1.049	33.572	-46.416	58.454	0.895	0.864
33.757	-38.198	71.728	0.830	1.060	33.757	-46.920	58.991	0.903	0.872
33.943	-38.966	72.518	0.839	1.072	33.943	-47.426	59.530	0.911	0.880
34.128	-39.732	73.306	0.848	1.084	34.128	-47.930	60.067	0.919	0.888
34.314	-40.501	74.098	0.857	1.095	34.314	-48.436	60.606	0.927	0.896
34.499	-41.267	74.886	0.866	1.107	34.499	-48.940	61.143	0.936	0.904
34.685	-42.036	75.677	0.875	1.119	34.685	-49.446	61.682	0.944	0.912
34.870	-42.802	76.465	0.884	1.130	34.870	-49.950	62.219	0.952	0.920
35.056	-43.571	77.256	0.894	1.142	35.056	-50.457	62.759	0.960	0.928
35.241	-44.337	78.044	0.903	1.154	35.241	-50.961	63.296	0.969	0.936
35.427	-45.103	78.832	0.912	1.165	35.427	-51.465	63.833	0.977	0.944
35.612	-45.872	79.623	0.921	1.177	35.612	-51.829	64.221	0.983	0.949
35.798	-46.637	80.411	0.930	1.189	35.798	-51.958	64.360	0.985	0.951
35.984	-47.406	81.202	0.939	1.200	35.984	-52.087	64.525	0.987	0.954
36.169	-48.17?	81.990	0.948	1.212	36.169	-52.235	64.748	0.991	0.957
36.355	-48.941	82.781	0.957	1.224	36.355	-52.312	64.956	0.994	0.960
36.540	-49.707	83.569	0.967	1.235	36.540	-52.344	65.152	0.997	0.963
36.726	-50.476	84.360	0.976	1.247	36.726	-52.305	65.349	1.000	0.966
36.975	-51.508	85.422	0.988	1.263					
36.985	-51.637	85.551	0.989	1.265					
36.975	-51.765	85.680	0.991	1.267					
36.898	-51.958	85.887	0.993	1.270					
36.814	-52.087	86.041	0.995	1.272					
36.654	-52.228	86.255	0.998	1.275					
36.461	-52.305	86.462	1.000	1.278					